Chapter 10

Wire target perturbations

10.1 Target design

mechanical schematic of target, room light image of target description of effect of wire array include image with wire shadows description of effect of glass support tubes, explain implantation of hydrogen, spectroscopic confirmation of light source include images of before and after really bright flare up, and graphs of corresponding spectra rotatablity magnetic probe access pros and cons of design

10.2 Observation of coherent density waves

This graph shows the location of observed plane waves and their approximate wavelength λ and direction. For some shots distinct waves were observed in multiple locations and so are listed separately. There was a noticeable amount of reproducibility of waves occurring in the same location, implying that the waves do not form at random, but instead are caused by some identifiable

mechanism.

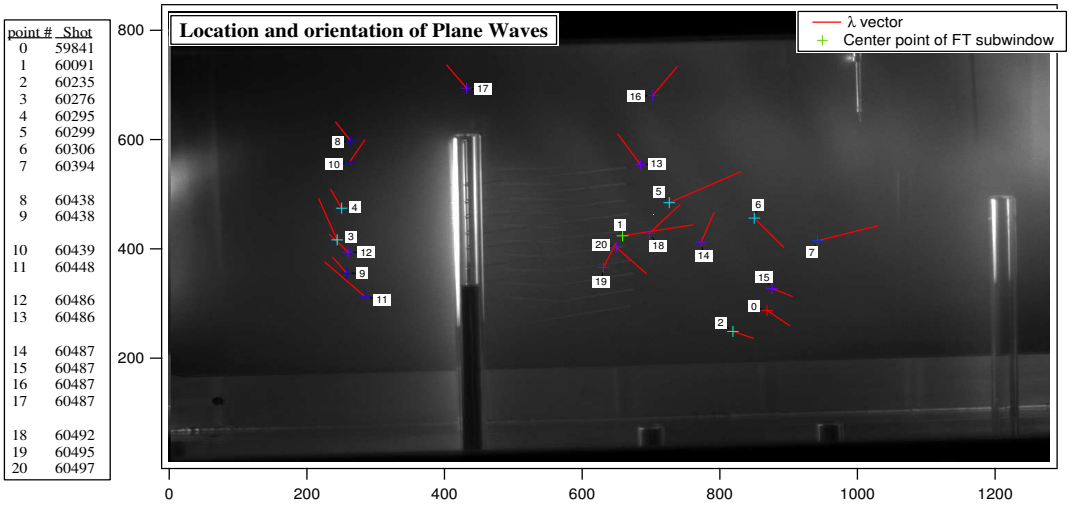

Figure 10.1: Plane wave locations with labels according to shot number.

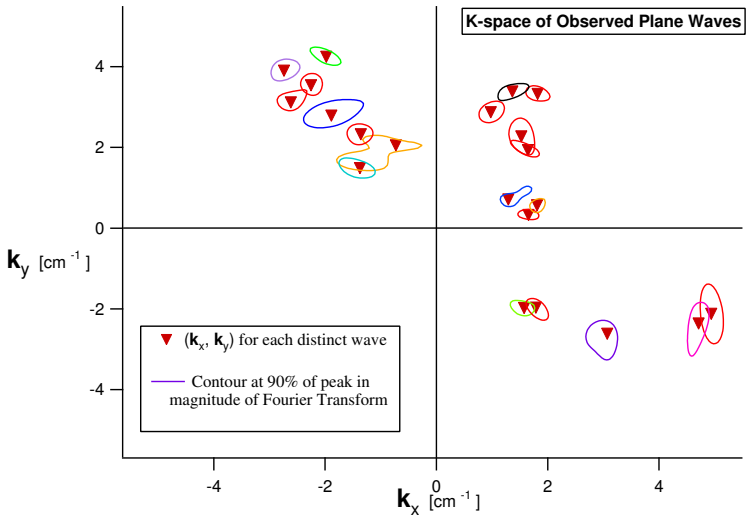

Figure 10.2: K-space distribution of Plane waves

Here are some examples of very localized Fourier modes, which we visually identify as plane waves. Shot 60438 Shot 60295 Shot 59841 Shot 60235

Exposure smear length is the distance the plasma should move during the camera exposure time (of 1 μs), based on time of flight measurements of plasma velocity.Here we compare this length to the wavelength of the plane waves.

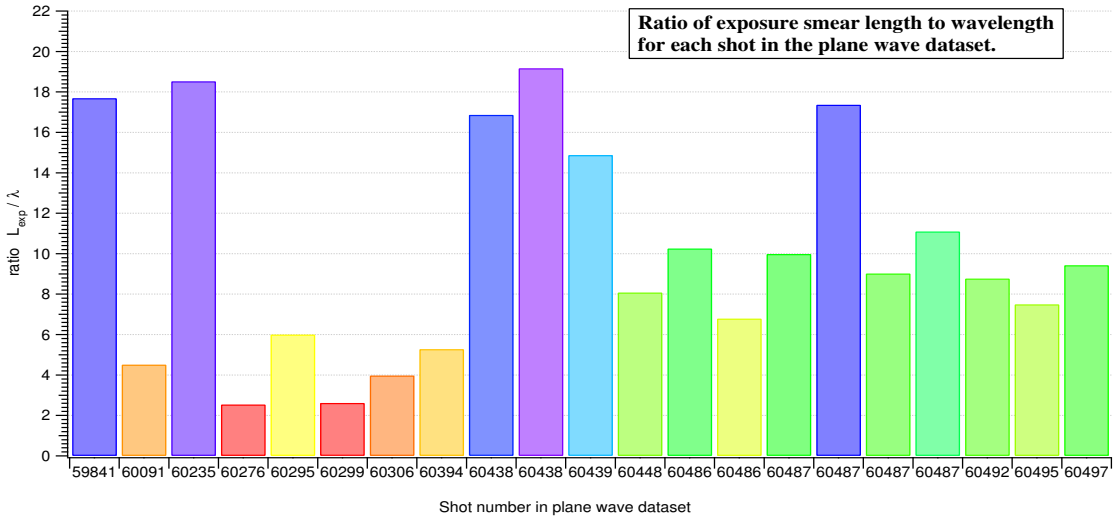

Figure 10.3: Ratio of expected exposure smear length to wavelength is displayed here vs shotnumber of data set.

The curious fact is that if these were plane waves that were co-moving with the plasma at a velocity between 3 to 15 $cm/\mu s$, then for an exposure of 1 full μs, we would not be able to resolve the clear wave structures on the order of 1 cm that we do see. If these were co-moving plane waves, the images would be mostly a blur do to the relatively long exposure time, and the fast motion of the plasma.We also see that there is no apparent trend that relates wavelength and plasma flow velocity, such as might be expected from a simple traveling wave with $\lambda f = v_\phi$This again implies that the wave speed is is not the same as the plasma flow speed.

The only viable conclusion is that these waves are essentially standing waves in the laboratory frame of reference, with wave velocities of no more than 1 $cm/\mu s$.The mechanism that is responsible for generating these density waves is not fully understood, however we have good reason to expect that the wire targets that were put in place with intention of causing measurable perturbations to the plasma did just that, and the result is that coherent, single-mode density waves

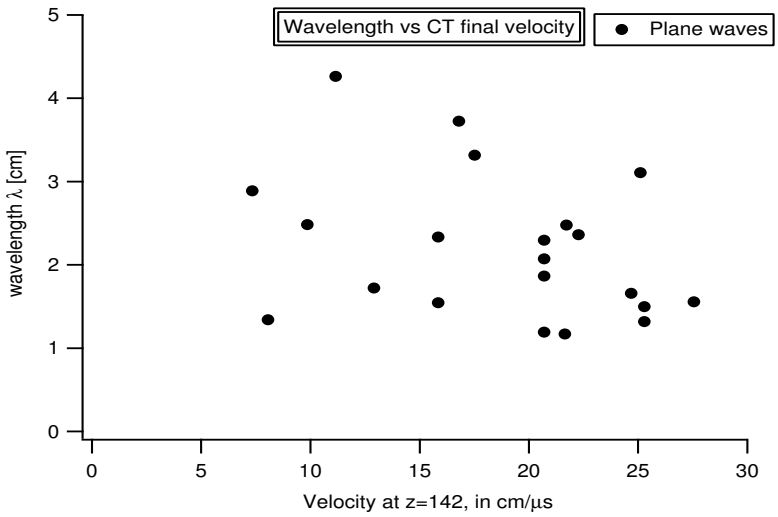

Figure 10.4: Wavelength vs plasma flow speed

are created if the plasmaconditions are right. Further analysis on the existing data is required to develop a better model of what causes these, and other wave phenomena in the CTIX plasma. Onereasonable model is that the electron density variation is due to the magnetic islands that form as the plasma passes through the wire array. Other possible mechanisms include,shock wave driven ion acoustic modes, or some sort of two stream instability between the moving CT plasma and a stationary singly ionized helium plasma. It is also worth noteing that more plane waves of the type discussed above were obserserved almost exclusively during target region gas puffing. In these shots the CT plasma collided with a stationary neutral population and the result was the apperance of coherent spatial variations in the total plasma luminosity. On the other hand, during shots with accelerator gas puffing, the neutrals had time to become ionized and acclerated by the fields by the time luminous regions of plasma crossed through the transverse viewing chamber. Images of the plasma during these shots had a fundamentally different character than those with the target region gas puffing.

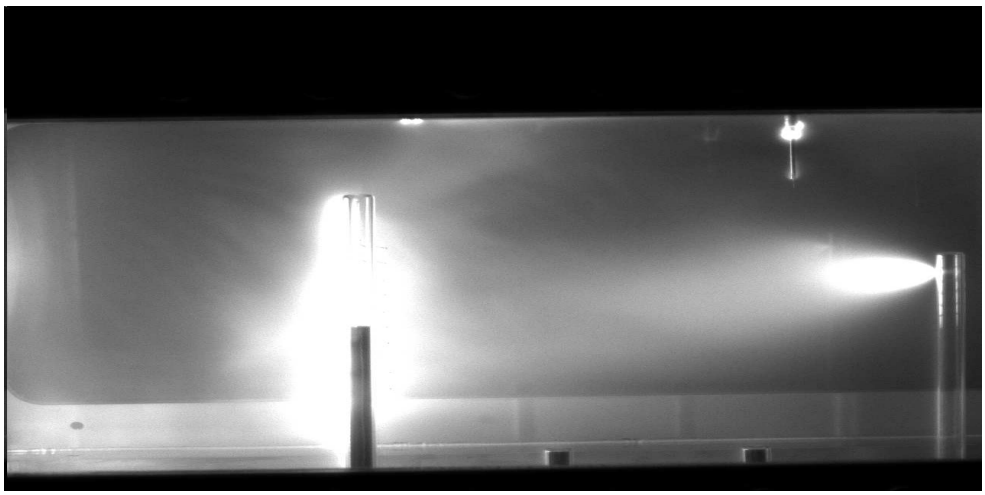

Figure 10.5: Coherent waves in plasma, USE BETTER EXAMPLES

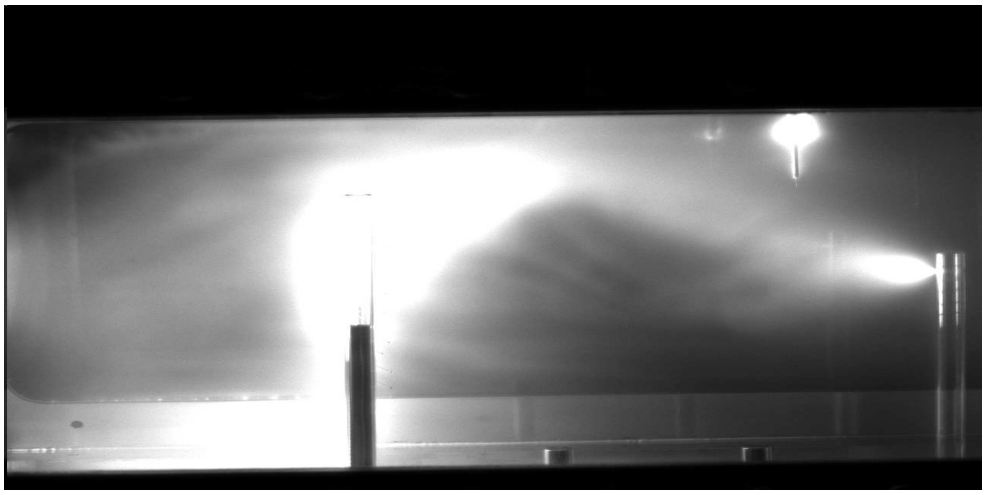

Figure 10.6: Coherent waves in plasma, USE BETTER EXAMPLES

10.3 Observation of turbulent waves

Observation of turbulence during accelerator region gas puff experiments One mode of operation was found to be especially useful for visualizing turbulent flow in the plasma. For example,

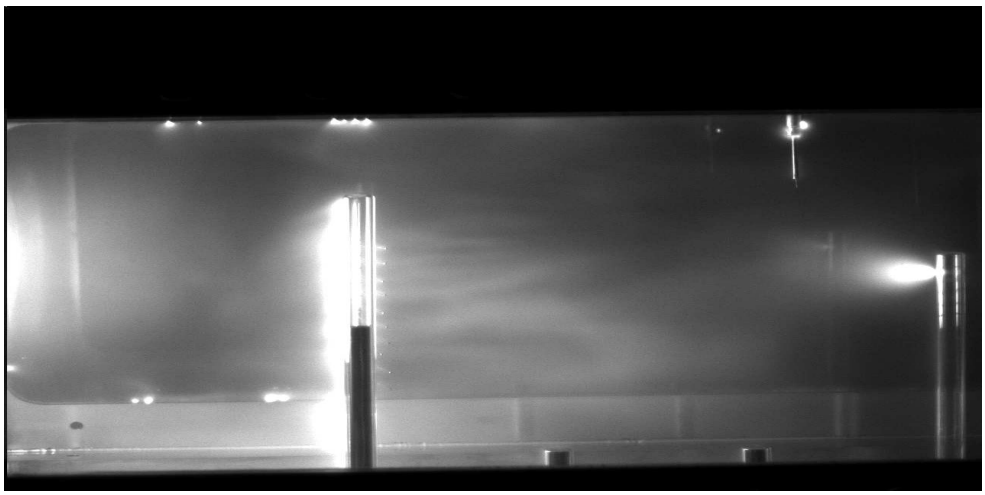

Figure 10.7: Coherent waves in plasma, USE BETTER EXAMPLES

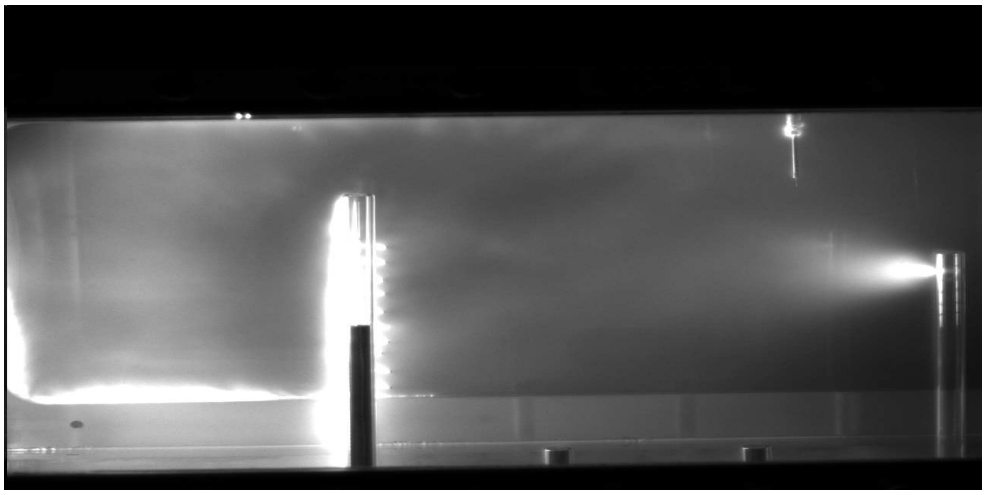

Figure 10.8: Coherent waves in plasma, USE BETTER EXAMPLES

the image taken on CTIX Shot 60062 (Fig 10.10) displays an apparent transition from laminar to turbulent flow as plasma passes wire target and support tubes, traveling from left to right.

The camera exposure for this shot was 1 μs, with a delay of 30 μs from the formation of the CT plasma. This image is of the relatively uniform B_θ pushing field plasma behind the CT, after the

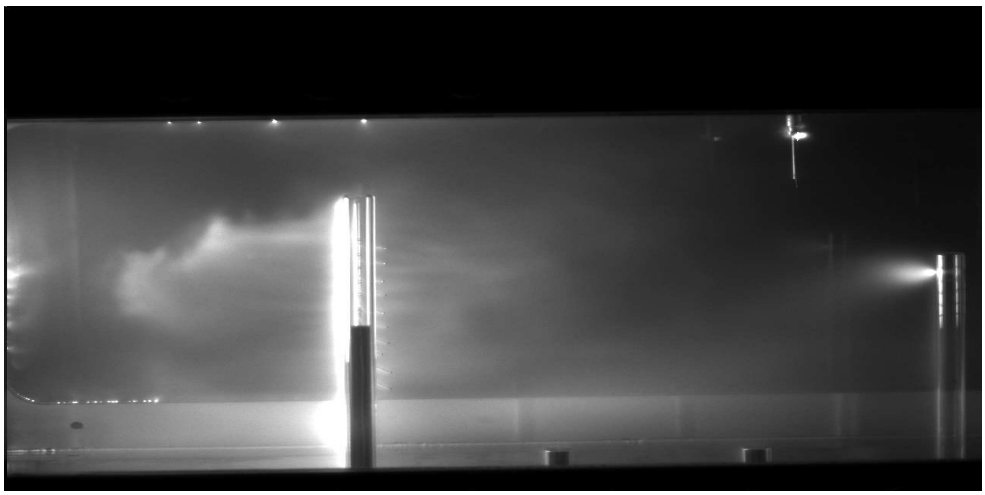

Figure 10.9: Coherent waves in plasma, USE BETTER EXAMPLES

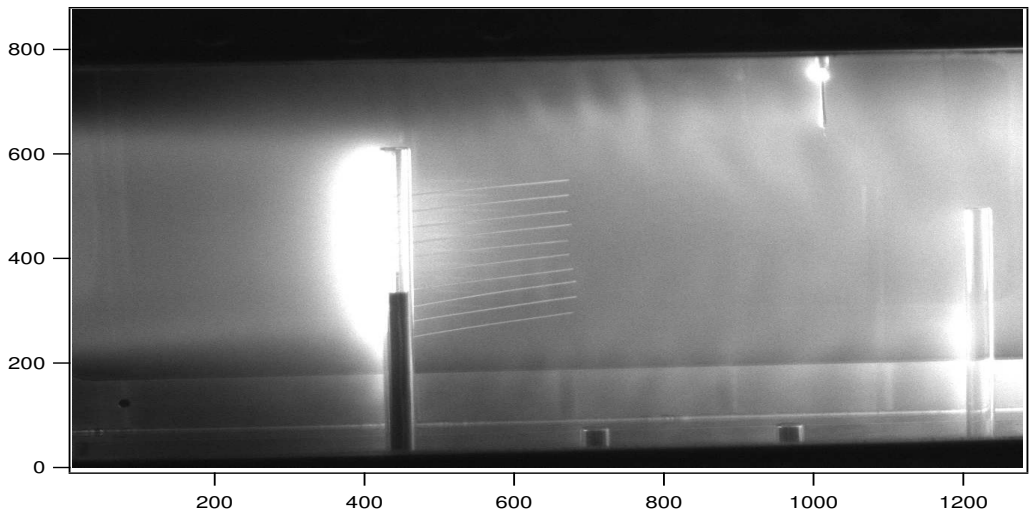

Figure 10.10: Transition to turbulent flow

CT has already moved through the viewing chamber. The helium gas puff was injected into the z = 91 cm accelerator port at approximately 14 milliseconds before the shot, which primarily served to increase the plasma electron density by about a factor of 3 for this shot. The secondary effect of the gas puffing is that helium ions (which serve as the dominant source of light for fast imaging) have

a chance to be captured and accelerated by the magnetic fields. By the time they enter the drift section they are co-moving with the plasma and therefore the light emission from these captured ions is indicative of the structure of the flow, and evidence of density fluctuations. When gas puff conditions are just right, this mode of operation is ideal for flow visualization, roughly analogous to using smoke to trace streamlines in wind-tunnel experiments. Injection velocity of SCT for this shot was 3.35 cm/μsDominant wavelength of post-target fluctuations for this shot was 2.5 cm.

Top graph in Figure 10.3 10.3 is the FT of the plasma flow in the region before it has interacted with the target. Bottom graph is the FT of the plasma after it has interacted with the target. The color scale represents the magnitude of the FT for any given wavevector (kx, ky), and the units are arbitrary, but the same for both top and bottom graphs.A significant increase in fluctuation amplitude is observed, as well as wider distribution of waves in the ky direction. Also the k-spectrum is noticeably more choppy and irregular for the turbulent flow than for the incoming laminar flow. The dominant wave modes in the turbulent spectrum are localized near k = (2.5, 0) [1/cm], where k = $2\pi/\lambda$. A custom-made discrete Fourier transform algorithm was used instead of a prepackaged FFT algorithm in order to provide more precise control of the resulting resolution in k space. Here are a few other nice examples of apparent laminar-turbulent transition. The time at which the images were taken are listed in parentheses. Shot 60053 (26 μs) Shot 60061 (27 μs) Shot 60055 (30 μs) Shot 60091 (27 μs)

10.4 Comparison of experimental results with plasma turbulence theory

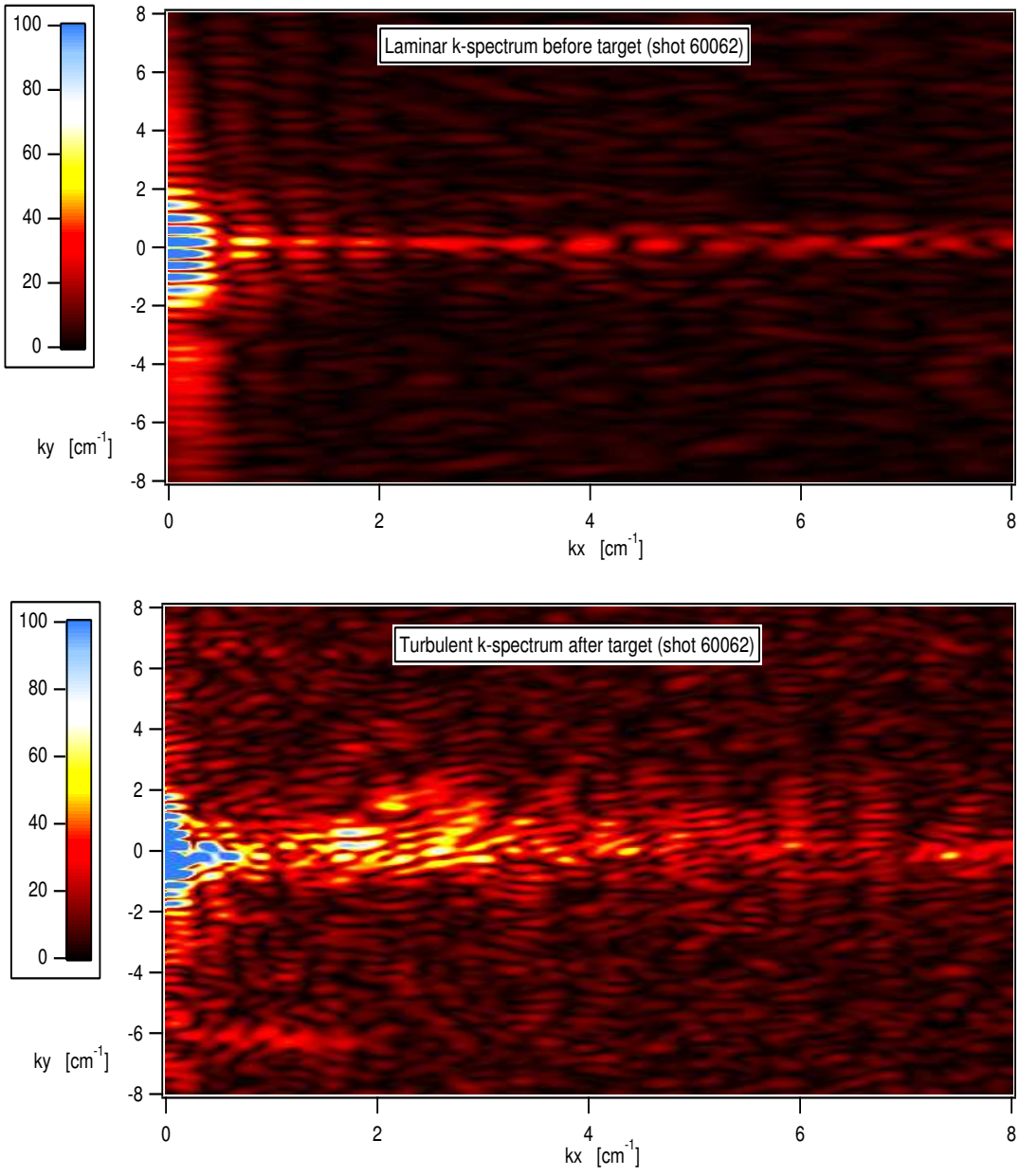

Figure 10.11: Fourier transforms of the image taken for shot 60062,(top) in laminar region before plasma has interacted with target, (bottom) turbulence after interaction.